ChemComm

ROYAL SOCIETY OF CHEMISTRY

COMMUNICATION

View Article Online
View Journal | View Issue

Open Access Article. Published on 26 October 2022. Downloaded on 11/4/2025 2:24:07 AM.
This article is licensed under a Creative Commons Attribution-NonCommercial 3.0 Unported Licence.

Check for updates

Cite this: *Chem. Commun.*, 2022, **58**, 12728

Received 18th July 2022,
Accepted 24th October 2022

DOI: 10.1039/d2cc04008e

rsc.li/chemcomm

The eutectic point in choline chloride and ethylene glycol mixtures†

Hannah J. Hayler and Susan Perkin *

The choline chloride (ChCl) and ethylene glycol (EG) mixture has become established as a paradigmatic deep eutectic solvent (DES). Here, we present measurements of the phase behaviour of this mixture over a wide composition range, and provide an extended phase diagram. The eutectic point was found to lie at −28 ± 1 °C and 0.01 < x_{ChCl} < 0.02, sharply contrasting with the previously expected eutectic composition. Our observations confirm that the eutectic temperature is not 'deep' compared to the ideal solution theory prediction. We also observe a cold-crystallisation at T = −65 °C which may have been formerly misinterpreted as the eutectic point.

Deep eutectic solvents (DESs) were first reported in 2001 by Abbott *et al.*[1] and their properties are frequently compared to those of ionic liquids (ILs). ILs and DESs have similar physical properties including tunability, wide liquidus ranges, and thermal stability.[2] Depending on the components used, DESs can also have advantages over ILs including biodegradability, non-toxicity, and ease of manufacture from inexpensive starting materials.[3] In fact, compared to ILs, DESs have been classed as more 'green' solvent alternatives[4,5] that can be used in synthesis,[6] metal processing applications like electrodeposition,[2] and as lubricants.[7–10]

Their name originates from their phase behaviour at the eutectic composition where the freezing point depression exceeds that predicted by ideal solution theory,[11] making most DESs liquid below approximately 150 °C.[3] At the eutectic composition, the mixture is frustrated from solidifying due to the presence of large, asymmetric ions and/or strong hydrogen bonding between the components. The former is also used to explain the phase behaviour of room-temperature ILs.[12] DESs are most commonly formed from the complexation of a quaternary ammonium salt and a hydrogen bond donor (*e.g.* amides, polyols, polyacids).[2] At the eutectic composition, the favourable hydrogen bonding interactions formed in the mixed liquid phase are stronger than the interactions in the individual component phases,[13] resulting in a finite negative contribution to the enthalpy of mixing, which depresses the freezing point and widens the liquidus range.

Choline chloride (ChCl) and ethylene glycol (EG) mixtures have been suggested to form a DES at an EG mole fraction, x_{EG}, of 0.667 *i.e.* 1 : 2 ChCl : EG, with a reported freezing point of T_f = −66 °C (Fig. 1, black full circles).[14] The 1 : 2 ratio has been rationalised by suggesting a favourable IL-like structure of choline cations and chloride-EG anionic 'complexes', where a

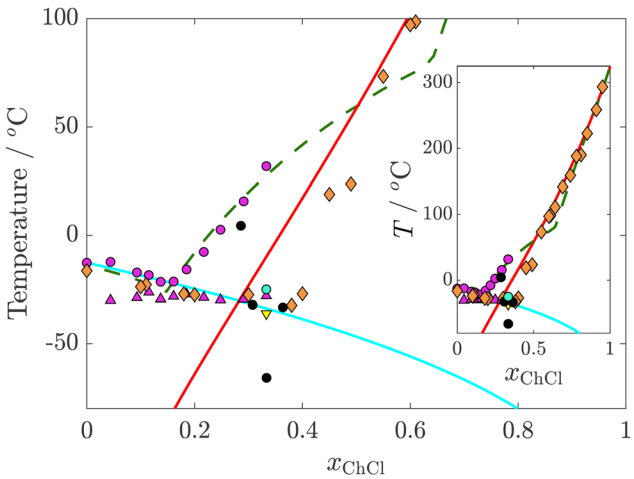

Fig. 1 Summary of previously reported temperature-composition (mole fraction of ChCl, $x_{ChCl} = 1 - x_{EG}$) phase behaviour for the ChCl : EG system. Ibrahim *et al.*[20] – yellow triangle; Crespo *et al.*[21] – green dashed line; Agieienko and Buchner[22] – magenta triangles and circles highlight the solidus and liquidus lines, respectively; Silva *et al.*[15] – orange diamonds; Shahbaz *et al.*[14] – black circles; Jani *et al.*[23] – cyan circle. Ideal solution liquidus lines calculated for ethylene glycol (cyan solid line) and choline chloride (red solid line) using eqn (1). For ethylene glycol, $\Delta_{fus}H$ = 9960 J mol^{-1} and T^* = −12.69 °C.[24] For choline chloride, $\Delta_{fus}H$ = 4300 ± 600 J mol^{-1} and T^* = 324 ± 7 °C.[25]

Physical and Theoretical Chemistry Laboratory, University of Oxford, South Parks Road, Oxford, OX1 3QZ, UK. E-mail: susan.perkin@chem.ox.ac.uk

† Electronic supplementary information (ESI) available. See DOI: https://doi.org/10.1039/d2cc04008e

This journal is © The Royal Society of Chemistry 2022

Open Access Article. Published on 26 October 2022. Downloaded on 11/4/2025 2:24:07 AM.
This article is licensed under a Creative Commons Attribution-NonCommercial 3.0 Unported Licence.

chloride ion is chelated by two EG molecules.[13] Since the work of Shahbaz *et al.*,[14] the eutectic temperature of 1 : 2 ChCl : EG has regularly been cited as −66 °C.[3,8,15–19]

However, this simplistic view of the DES structure continues to be questioned and proper understanding of the system is hampered by relative lack of direct measurements of phase behaviour. Recently, several reports of the ChCl : EG mixture revealed contrasting observations; we collate these in Fig. 1. Ibrahim *et al.*[20] suggest T_f = −36 °C (Fig. 1, yellow triangle). Silva *et al.*[5] observe a solidus line at roughly −32 °C and eutectic composition of x_{EG} = 0.62 (Fig. 1, orange diamonds), with no deviation from ideality *i.e.* ideal solution theory is applicable. Phase diagrams of ChCl : EG and water mixtures were presented by Jani *et al.*,[23] wherein dry 1 : 2 ChCl : EG showed a single exothermic peak at −25 °C (Fig. 1, cyan circle). Using statistical associating fluid theory (SAFT)-type equations, Crespo *et al.*[21] model the solid-liquid equilibrium behaviour of ChCl : EG yielding a eutectic point at $x_{EG} > 0.8$ and $T_f \approx -33$ °C (Fig. 1, green dashed line). A less negative eutectic temperature of $T_f \approx -29$ °C was also observed recently by Agieienko and Buchner *et al.*[22] at $x_{EG} \approx 0.83$ (Fig. 1, magenta circles and triangles). They conclude that 1 : 2 ChCl : EG is not the eutectic composition, and that the depression of the freezing point at $x_{EG} \approx 0.83$ (1 : 4.85 ChCl : EG) is not significantly different from ideal behaviour implying that the eutectic mixture is not a DES.[22] For comparison to ideal solution theory, in Fig. 1 we also show the ideal solution liquidus lines for the individual components, EG and ChCl, in cyan and red respectively. These are calculated from the following expression:

$$T = \frac{T^* \Delta_{fus} H}{\Delta_{fus} H - RT^* \ln x_A}, \quad (1)$$

which describes how the freezing point of the mixture, T, varies from the freezing point of pure A, T^*, depending on the the mole fraction x_A and the enthalpy of fusion $\Delta_{fus}H$. R is the molar gas constant.

Here we report measurements of phase transitions in ChCl : EG mixtures across a wide range of compositions, contributing to and extending the phase diagram. We find that (i) the eutectic point lies at −28 °C and in the range $0.01 < x_{ChCl} < 0.02$; (ii) for $x_{ChCl} > 0.02$ the mixture still had a solid nature up to high temperatures and undergoes a solid–solid transition between two crystalline states at 77 °C; and (iii) at temperatures much lower than the eutectic point a kinetic solid–solid transition could be recorded which may have previously been misinterpreted as the thermodynamic eutectic point. Experimental methods are discussed in detail in the ESI.†

Using differential scanning calorimetry (DSC), three distinct types of thermal transition were observed, examples of which are shown in Fig. 2. These transitions were used to construct the phase diagram in Fig. 3. Firstly, the leftmost exothermic peak observed at approximately −65 °C in samples with mole fraction $0.01 < x_{ChCl} < 0.79$ (Fig. 2(a)) is attributed to the cold–crystallisation (c–c) of the sample. A second c–c peak is also observed at approximately −46 °C in samples with mole fraction $0.08 < x_{ChCl} < 0.6$.

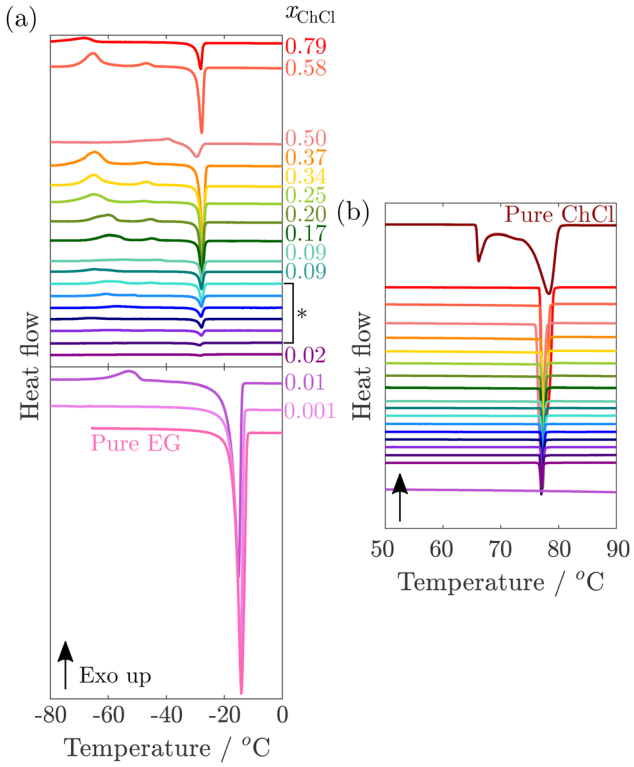

Fig. 2 Heating DSC scans (offset vertically for clarity) for ChCl and EG mixtures at different compositions (a) below 0 °C and (b) above 50 °C. No thermal events were observed between 0 °C and 50 °C. All samples were heated at 1 °C min^{-1}. The arrows indicate the direction of exothermic (*exo*) transitions. In both plots, scans from top to bottom show decreasing ChCl content. The corresponding ChCl mole fractions, x_{ChCl}, are labelled in (a). Within the region marked by (*), the six thermograms correspond to x_{ChCl} = 0.08, 0.07, 0.06, 0.05, 0.04, 0.03.

The second thermal transition of interest is the endotherm observed between −30 and −10 °C. In pure EG, this corresponds to the melting point of EG. On addition of ChCl, this peak shifts to lower temperatures before converging at approximately −28 °C, which we attribute to the eutectic melting point (see ESI,† for Tammann plot). Finally, the rightmost endotherm observed at 77 °C in samples with mole fraction $x_{ChCl} > 0.01$ (Fig. 2(b)), corresponding to the solid–solid transition[26] (s–s trs) observed when the crystal structure of ChCl changes from orthorhombic (α-ChCl) to face-centred cubic (β-ChCl).[27]

To produce the phase diagram in Fig. 3, we have taken the peak temperatures of the c–c transitions, and the onset temperatures of the melts and s–s transitions (see ESI† for further details). At the lowest temperatures studied, we observe a c–c at approximately −65 °C for samples with mole fraction $0.01 < x_{ChCl} < 0.79$. A second c–c peak is also observed at approximately −46 °C in samples with mole fraction $0.08 < x_{ChCl} < 0.6$. As the temperature is increased, a melting transition occurs. When $x_{ChCl} > 0.02$ the melting point is −28 ± 1 °C (see Fig. 3). However, when $x_{ChCl} < 0.01$, the observed melting point increases and is more comparable to that of pure EG.[28] For $x_{ChCl} > 0.02$, we also observe a s–s transition at 77 °C, characteristic of the change from α to β-ChCl.[26] Using these transitions, we suggest a liquidus line given by the grey lines in

Open Access Article. Published on 26 October 2022. Downloaded on 11/4/2025 2:24:07 AM.
This article is licensed under a Creative Commons Attribution-NonCommercial 3.0 Unported Licence.

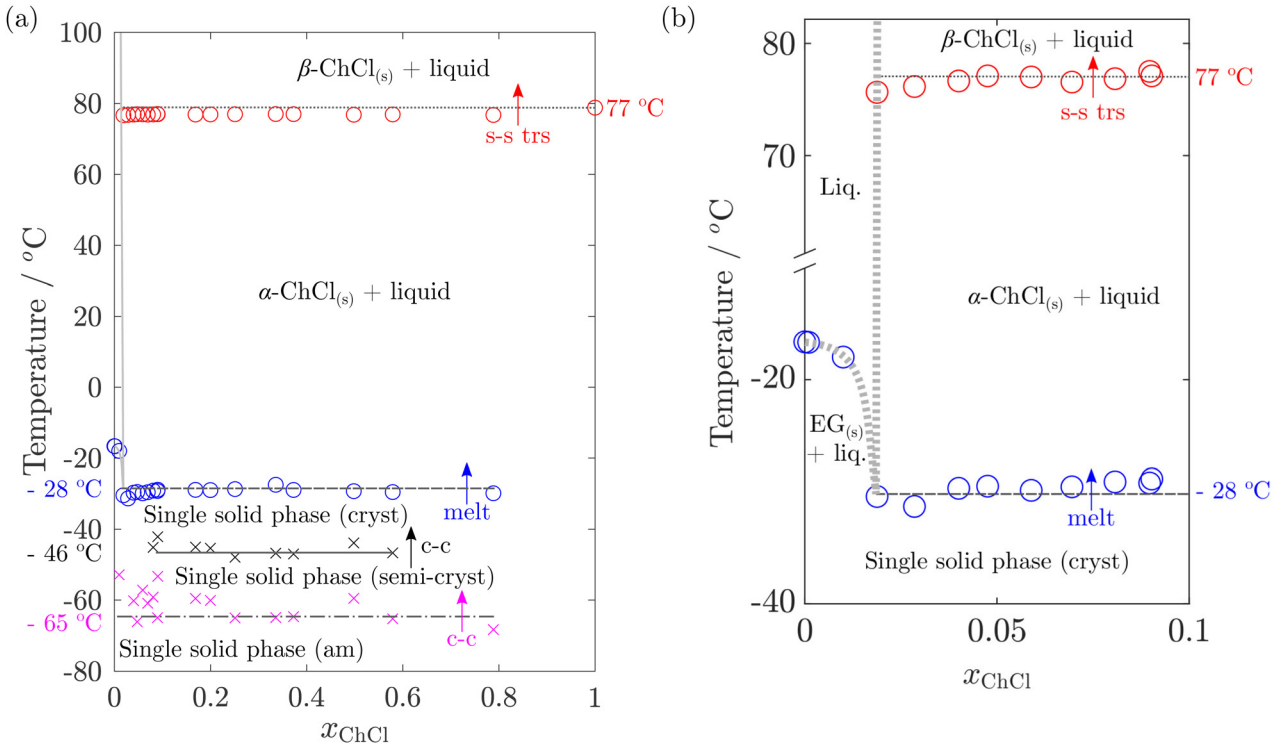

Fig. 3 Empirical temperature-composition (mole fraction of ChCl, x_{ChCl}) phase diagram for the ChCl : EG system (a) over the full composition range, and (b) in the region where $x_{ChCl} < 0.1$. The thermal events observed in Fig. 2 are plotted: cold–crystallisations (c–c, pink & black), melt (blue), solid–solid transition (s–s trs, red). Onset and peak temperatures are plotted as open circles and crosses, respectively. All lines are guides to the eye indicating the regions delineated by the measured data points. We highlight seven different regions: amorphous (am) single solid phase (below black dot-dashed line); semi-crystalline (semi-cryst) single solid phase (between dot-dashed and solid black lines); crystalline (cryst) single solid phase (between solid and dashed black lines); solid α–ChCl + liquid two phase region (between dashed and dotted black lines); solid β–ChCl + liquid two phase region (above dotted black line); single liquid (Liq.) phase (above grey dashed line in (b)); solid EG + liquid two phase region (below the grey dashed line in (b)). Measurement of the solid–solid transition at $x_{ChCl} \approx 0.02$ constrains the eutectic point to $0.01 < x_{ChCl} < 0.02$.

Fig. 3(a) and (b), and a eutectic point between $0.01 < x_{ChCl} < 0.02$. Above the proposed liquidus line we suggest a single liquid phase. Between the solidus (−28 °C) and liquidus lines, we suggest two two-phase regions (see Fig. 3(b)). To the left of the eutectic composition, a region of solid EG + liquid, and to the right, a solid α-ChCl + liquid region.

Interestingly, on inspecting our ChCl : EG phase diagram (Fig. 3), we observe features which connect and help to interpret the works of Shahbaz *et al.*,[14] Agieienko and Buchner,[22] and Gilmore *et al.*[29] The bulk phase behaviour of ChCl : EG mixtures does not show a eutectic melt at −66 °C and a 1 : 2 ChCl : EG composition as reported by Shahbaz *et al.*;[14] instead we observe a cold-crystallisation at this temperature. The eutectic melt we observe supports the work of Agieienko and Buchner[22] where a solidus line is observed at −29 °C, although our eutectic composition is found at lower x_{ChCl} compared to Agieienko and Buchner.[22] The work of Agieienko and Buchner[22] studies the thermal transitions below $T_{max} \approx 50$ °C. As our measurements probe higher temperatures, we also observe the ChCl solid–solid transition when x_{ChCl} is greater than the eutectic composition, also observed by Gilmore *et al.*[29] in the ChCl : Urea phase diagram for x_{ChCl} = 0.45–0.90. We note that constructing the ChCl : EG phase diagram from DSC measurements was not trivial and involved considering both thermodynamic and kinetic transitions. Future improvements to the phase diagram would benefit from the combination of DSC measurements such as these with additional techniques; for example polarised optical microscopy as applied by Gilmore *et al.*[29] in identifying the ChCl : Urea phase transition points.

In summary, we show that the eutectic melt of ChCl : EG is at −28 °C, corroborating recent work of Agieienko and Buchner,[22] and that the eutectic composition is constrained to $0.01 < x_{ChCl} < 0.02$. These values do not coincide with those reported by Shahbaz *et al.*[14] at −66 °C and 1 : 2 ChCl : EG, and more generally our study of ChCl : EG mixtures using DSC highlights the importance of careful separation of thermodynamic and kinetic transitions near eutectic points. In fact, a cold-crystallisation transition was found around −66 °C. However, crystallisation is usually under kinetic control whereas the measured melting points are thermodynamic; empirical freezing and melting points are rarely equal. Within the DES community, a clearer definition of a 'deep eutectic solvent' is required that does not only depend on kinetic thermal behaviour *i.e.* a depression in the freezing point. A revised definition should be thermodynamically unambiguous as well as providing a clear empirical route for classification.

The authors gratefully acknowledge funding from the European Research Council (under Consolidator Grant No. 101001346, ELECTROLYTE).

 This journal is © The Royal Society of Chemistry 2022

Open Access Article. Published on 26 October 2022. Downloaded on 11/4/2025 2:24:07 AM.
This article is licensed under a Creative Commons Attribution-NonCommercial 3.0 Unported Licence.

Conflicts of interest

There are no conflicts to declare.

References

1 A. P. Abbott, G. Capper, D. L. Davies, H. L. Munro, R. K. Rasheed and V. Tambyrajah, *Chem. Commun.*, 2001, 2010–2011.
2 E. L. Smith, A. P. Abbott and K. S. Ryder, *Chem. Rev.*, 2014, **114**, 11060–11082.
3 Q. Zhang, K. D. O. Vigier, S. Royer and F. Jérôme, *Chem. Soc. Rev.*, 2012, **41**, 7108–7146.
4 A. Paiva, R. Craveiro, I. Aroso, M. Martins, R. L. Reis and A. R. C. Duarte, *ACS Sustainable Chem. Eng.*, 2014, **2**, 1063–1071.
5 L. P. Silva, M. A. Martins, J. H. Conceição, S. P. Pinho and J. A. Coutinho, *ACS Sustainable Chem. Eng.*, 2020, **8**, 15317–15326.
6 E. R. Cooper, C. D. Andrews, P. S. Wheatley, P. B. Webb, P. Wormald and R. E. Morris, *Nature*, 2004, **430**, 1012–1016.
7 S. D. Lawes, S. V. Hainsworth, P. Blake, K. S. Ryder and A. P. Abbott, *Tribol. Lett.*, 2010, **37**, 103–110.
8 A. P. Abbott, E. I. Ahmed, R. C. Harris and K. S. Ryder, *Green Chem.*, 2014, **16**, 4156–4161.
9 E. I. Ahmed, A. P. Abbott and K. S. Ryder, Lubrication studies of some type III deep eutectic solvents (DESs), AIP Conf. Proc., 2017, vol. 1888, p. 020006.
10 I. Garcia, S. Guerra, J. de Damborenea and A. Conde, *Lubricants*, 2019, **7**, 37.
11 M. A. Martins, S. P. Pinho and J. A. Coutinho, *J. Solution Chem.*, 2019, **48**, 962–982.
12 M. V. Fedorov and A. A. Kornyshev, *Chem. Rev.*, 2014, **114**, 2978–3036.
13 O. S. Hammond, D. T. Bowron and K. J. Edler, *Green Chem.*, 2016, **18**, 2736–2744.
14 K. Shahbaz, F. S. Mjalli, M. Hashim and I. M. ALNashef, *J. Appl. Sci.*, 2010, **10**, 3349–3354.
15 K. Shahbaz, S. Baroutian, F. S. Mjalli, M. A. Hashim and I. M. AlNashef, *Thermochim. Acta*, 2012, **527**, 59–66.
16 K. Shahbaz, F. S. Mjalli, M. A. Hashim and I. M. AlNashef, *Fluid Phase Equilib.*, 2012, **319**, 48–54.
17 F. S. Bagh, K. Shahbaz, F. S. Mjalli, I. M. AlNashef and M. A. Hashim, *Fluid Phase Equilib.*, 2013, **356**, 30–37.
18 Z. Chen, B. McLean, M. Ludwig, R. Stefanovic, G. G. Warr, G. B. Webber, A. J. Page and R. Atkin, *J. Phys. Chem. C*, 2016, **120**, 2225–2233.
19 S. J. Bryant, A. J. Christofferson, T. L. Greaves, C. F. McConville, G. Bryant and A. Elbourne, *J. Colloid Interface Sci.*, 2022, **608**, 2430–2454.
20 R. K. Ibrahim, M. Hayyan, M. A. AlSaadi, S. Ibrahim, A. Hayyan and M. A. Hashim, *J. Mol. Liq.*, 2019, **276**, 794–800.
21 E. A. Crespo, L. P. Silva, J. O. Lloret, P. J. Carvalho, L. F. Vega, F. Llovell and J. A. Coutinho, *Phys. Chem. Chem. Phys.*, 2019, **21**, 15046–15061.
22 V. Agieienko and R. Buchner, *Phys. Chem. Chem. Phys.*, 2022, **24**, 5265–5268.
23 A. Jani, T. Sohier and D. Morineau, *J. Mol. Liq.*, 2020, **304**, 112701.
24 D. R. Lide, *CRC Handbook of Chemistry and Physics*, CRC Press, Boca Raton, FL, 84th edn, 2003.
25 L. Fernandez, L. P. Silva, M. A. Martins, O. Ferreira, J. Ortega, S. P. Pinho and J. A. Coutinho, *Fluid Phase Equilib.*, 2017, **448**, 9–14.
26 I. M. Aroso, A. Paiva, R. L. Reis and A. R. C. Duarte, *J. Mol. Liq.*, 2017, **241**, 654–661.
27 R. L. Collin, *J. Am. Chem. Soc.*, 1957, **79**, 6086.
28 D. R. Cordray, L. R. Kaplan, P. M. Woyciesjes and T. F. Kozak, *Fluid Phase Equilib.*, 1996, **117**, 146–152.
29 M. Gilmore, M. Swadzba-Kwasny and J. D. Holbrey, *J. Chem. Eng. Data*, 2019, **64**, 5248–5255.